ARTICLE

Recycling of multilayer packaging using a reversible cross-linking adhesive

Katharina M. A. Kaiser[1,2] (ORCID)

[1]TUM School of Life Sciences Weihenstephan, Technical University of Munich, Freising, Germany

[2]Process Development for Polymer Recycling, Fraunhofer Institute for Process Engineering and Packaging IVV, Freising, Germany

Correspondence
Katharina M. A. Kaiser, TUM School of Life Sciences Weihenstephan, Technical University of Munich, Weihenstephaner Steig 22, 85354 Freising, Germany.
Email: katharina.kaiser@ivv.fraunhofer.de

Abstract

Plastic-based multilayer packaging has an important function on the packaging market, but is currently not recyclable as the polymer layers used are usually thermodynamically immiscible. This work therefore follows the approach to prepare separable multilayer packaging using a packaging adhesive modified with thermally unstable adducts, and proposes a corresponding recycling process. For this purpose, typical multilayer structures (polyethylene (PE)// polyethylene terephtalate (PET), PET//aluminum, and PE//aluminum) were prepared by curing furan-/maleimide-functionalized polyurethane (PU)-prepolymers with a three-functional cross-linking agent. Adhesions of up to over 3N per 15 mm test specimen were measured or substrate failures of PET films were observed. However, heating in dimethylsulfoxide, the retro-Diels–Alder reaction takes place and the cross-linked adhesive turns thermoplastic and dissolves in the solvent. Thus, the laminate separates and the pure PE, PET, and aluminum foils can be recovered without any PU residue.

KEYWORDS

addition polymerization, adhesives, packaging, polyurethane

1 | INTRODUCTION

According to the European Plastics Strategy, all packaging used should be reusable or recyclable by 2030.[1] At present, multilayer packaging, in which different materials are combined in a layered structure, represents the largest proportion of nonrecyclable packaging, accounting for around 20% of all flexible packaging.[2] The reason for the high proportion of multilayer packaging is that the combination of different materials allows tailor-made property profiles to be created with low material consumption.[3] Defined barrier properties against oxygen, water vapor, light, or loss of aroma enable long shelf lives and thus enable the current form of food trade and also reduce food losses.[4] Since in many cases the different polymers/materials are immiscible, these packagings usually cannot be recycled. Additionally, the current recycling systems aims at the recycling of monomaterials and multilayer packaging is sorted out and sent to incineration.[5]

Accordingly, in order to increase the recycling rates for polyethylene (PE), polypropylene (PP), polyethylene terephthalate (PET), and aluminum, new recycling strategies are required to handle multilayer materials and other composites. To address this problem from the packaging design side, it is one option to replace heterogeneous multilayer packaging with packaging consisting of different PE and/or PP types and thus to produce a type of monomaterial packaging. In this way, however, it is often not

possible to generate the material properties that are usually achieved with conventional multilayers, which can also have negative effects on the contents.[4,6] Another approach would be to connect the components of the multilayer packaging in such a way that the different materials can be separated again after their lifetime. The individual components could thus be recycled separately.[5]

Such "disjoinable" multilayer packaging can be achieved by using a thermoreversible cross-linked adhesive systems, which allows the separation of the laminates under defined conditions. After selective sorting of the multilayer packaging from postconsumer packaging waste, which is possible using new technologies,[7] the recycling rate could be increased in this way.

Reversible cross-linking can be achieved for example, by exposure to ultrasound, UV light, or heat.[8–15] An important example of such a thermo-responsive system is the Diels–Alder/retro-Diels–Alder (DA) equilibrium between furan and maleimide derivatives.[16–22] The major advantage of this system is the expedient temperature range of the [4 + 2] cycloaddition and the cycloreversion: the formation of the adduct starts at room temperature, but the reverse reaction requires temperatures of 90–130°C. The back reaction therefore takes place in a temperature range in which most conventional polymers are dimensionally stable. However, in the case of PE, for example, the retro-DA reaction would have to take place in a correspondingly low temperature range.[20]

Here, it is shown that multilayer packaging can be produced using laminating adhesives with reversible cross-links. Since cross-linked polyurethanes (PU) based on 4,4′-Methylene diphenyl diisocyanate (MDI) and polyester diols are frequently used for packaging adhesives,[23] the adhesive in this paper comprises PU prepolymers of different molecular weights functionalized with maleimide/furan derivatives and a cross-linking agent. Using these components PET//PE, PET//aluminum, and PE//aluminum laminates were produced; characterized; and the film materials PET, PE, and aluminum were recycled by temperature treatment in a solvent.

2 | EXPERIMENTAL

The method presented in this paper comprises the production of the laminates, the production of the individual adhesive components, and the recovery of the composite materials via a recycling process.

The adhesive polymers are linear polyester–PU prepolymers, functionalized with maleimide/furan moieties. In addition, a cross-linking molecule, containing three furan groups was synthesized using furfuryl glycidyl ether and a trithiol. Based on this, laminates are produced and cured. For recycling, the laminates are reduced in size (1 × 1 cm) and treated with a heated solvent (dimethylsulfoxide [DMSO], 105°C) under moderate stirring. This process allows opening of the DA adducts and subsequent solvation of the adhesive components. After this, the delaminated materials of the laminates can be sorted diversely, for example, by density separation, while the DMSO can be reused several times before it has to be distilled and the adhesive is discarded. An overview of the individual steps of the process is given in Figure 1. The exact procedure of these steps and a description of the syntheses are given in the following.

2.1 | Preparation of the adhesive

MDI (98%) was obtained from Alfa Aesar (Ward Hill, MA) and used as received. Furfuryl alcohol (FFA) (98%, Sigma–Aldrich, MO) was distilled prior to use, the diol Capa 2054 (Perstorp, Malmö, Sweden) is dried prior to use at reduced pressure at 50°C. The maleimide functional group, N-(2-hydroxyethyl)-maleimide (N-HEMI), is prepared with DA and retro-DA cycloaddition through a three steps process as described by Heo et al.[24] and Duan et al.[25] Ethyl acetate ($\geq$ 99.5%) was purchased from TH Geyer and, if necessary, dried with molecular sieve (4 Å) to a H_2O content < 50 ppm and stored under nitrogen ($H_2O \leq 50$ ppm). Reactions involving the use of MDI were carried out under a nitrogen atmosphere.

To produce the prepolymers, MDI was heated to 50°C to give a clear, colorless liquid to which Capa 2054 was added all at once. After the exothermic reaction subsided, the mixture was heated to 70°C until reaction control with Fourier transform infrared spectrometer (FTIR) showed no further decrease of the NCO-signal at 2260 cm^{-1}. For the preparation of furan-functionalized prepolymers, furfuryl alcohol, and eventually some ethyl acetate to ensure homogeneous mixing, was then added and the mixture was stirred at 70°C until the NCO-signal vanished. Possible residues of ethyl acetate were removed under reduced pressure. For the preparation of maleimide-functionalized prepolymers, N-HEMI was dissolved in ethyl acetate and then added to the mixture. The reaction was kept at 70°C until the NCO-signal vanished. Residues of ethyl acetate were removed under reduced pressure.

2.1.1 | Maleimide-functionalized prepolymers (1M–6M)

Infrared spectroskopy (IR) $\tilde{v}$ = 3,329 (br), 2,941 (m), 2,864 (m), 1,702 (s), 1,736 (s), 1,528 (s), 1,217 (s), 1,068 (s), 695 (intensity depends on molecular weight) cm^{-1}.
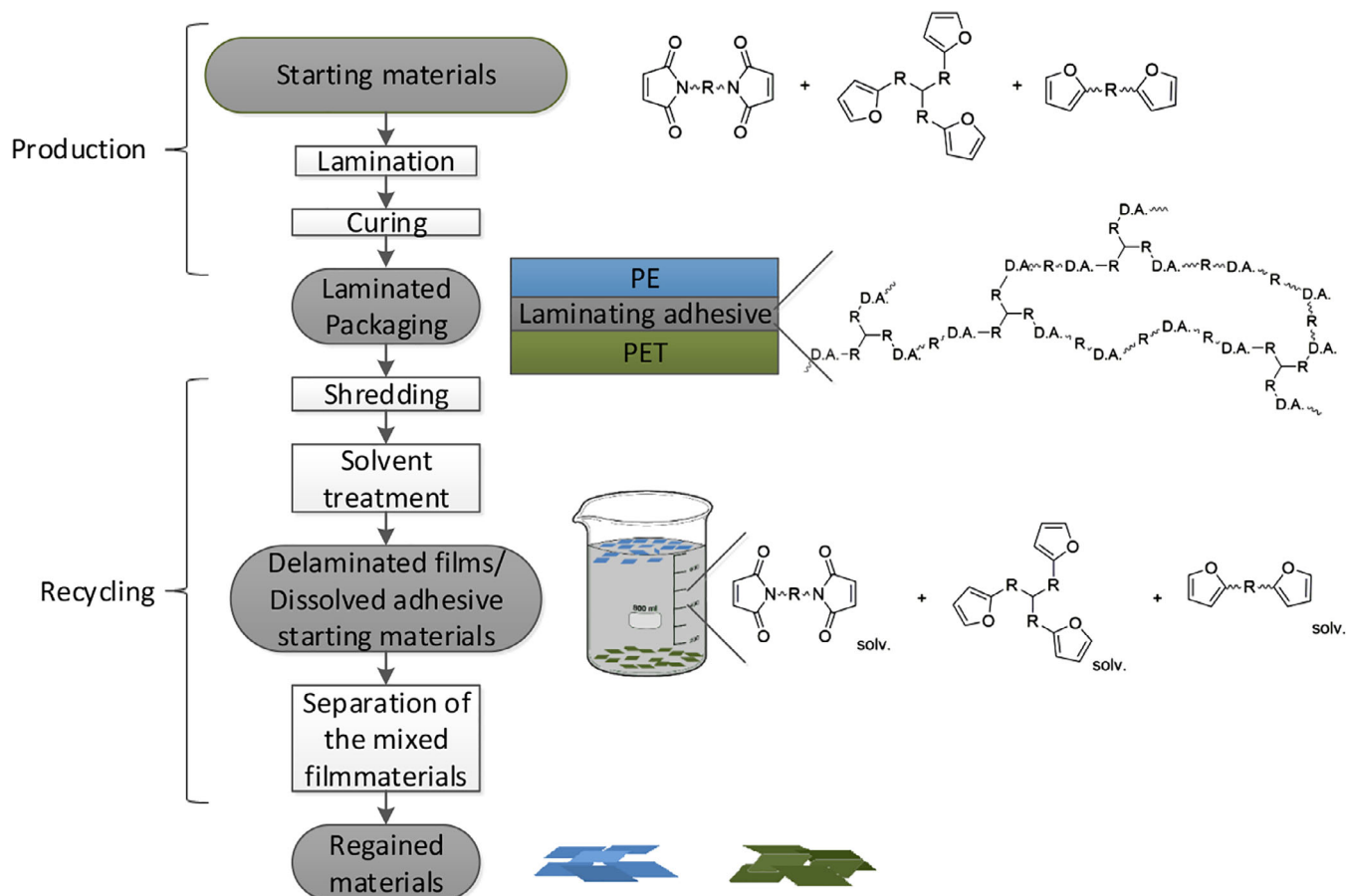
FIGURE 1 Overview of the complete laminate production and recycling process: PET//PE, PET//aluminum, PE//aluminum, and PET//PET laminates are produced starting from maleimide/furan-functionalized PU prepolymers of different molecular weights and a cross-linking molecule. For subsequent recycling, the laminates are shredded and treated with a heated solvent to induce the retro-Diels–Alder reaction and, subsequently, the dissolution of the adhesive components. Due to its low density, PE can be collected from the surface and thus be separated from PET or aluminum. R stands for the PU backbone of different chain lengths, formed from MDI and a polyester diol. D.A., Diels–Alder adduct [Color figure can be viewed at wileyonlinelibrary.com]

[1]H nuclear magnetic resonance (NMR) (300 MHz, DMSO-d_6) δ 9.74–9.38 (m; NH), 7.38–7.31 (m; Ar), 7.09–7.07 (m; Ar), 7.02 (4H; s; CH [N-HEMI]), 4.24–4.16 (m; CH_2 [polyester]), 4.15–4.08 (8H; m; CH_2 [N-HEMI]), 4.06–3.96 (m; CH_2 [polyester]), 3.78 (s; CH_2; [MDI]), 3.73–3.56 (m; CH_2 [polyester]), 2.31–2.24 (m; CH_2 [polyester]), 1.66–1.46 (m; CH_2 [polyester]), 1.37–1.27 (m; CH_2 [polyester]) (for details, see Appendix).

2.1.2 | Furan-functionalized prepolymers (1F–6F)

IR ṽ = 3,329 (br), 2,941 (m), 2,864 (m), 1,702 (s), 1,736 (s), 1,528 (s), 1,217 (s), 1,068 (s), 740 (intensity depends on molecular weight) cm^{-1}.

^{1}H NMR (300 MHz, DMSO-d_6) δ 9.71–9.40 (m; NH), 7.68 (2H; s; CH [FFA]), 7.37–7.33 (m; Ar), 7.17–7.01 (m; Ar), 6.50 (4H; dd; CH [FFA]), 5.09 (4H; s; CH_2

[FFA]), 4.18–4.09 (m; CH_2 [polyester]), 4.05–3.95 (m; CH_2 [polyester]), 3.78 (s; CH_2 [MDI]), 3.65–3.57 (m; CH_2 [polyester]), 2.30–2.23 (m; CH_2 [polyester]), 1.64–1.49 (m; CH_2 [polyester]), 1.39–1.23 (m; CH_2 [polyester]) (for details, see Appendix).

The cross-linker was made from furfuryl glycidyl ether (produced according to a prescription of Rostami et al.[21]) and trimethylolpropane tris(3-mercaptopropionate) according to a prescription of Habibi et al.[26] (see Appendix).

FTIR

For IR measurements, a Fourier transform infrared spectrometer (L1280034) with the software Spectrum One by Perkin Elmer (Shelton, CT) was used. The instrument used in this study was the ATR (Golden Gate, Perkin Elmer, Shelton, CT) device. For one spectrum, 10 scans were recorded. The wavenumbers in the mid-infrared region range from 4,000 to 600 cm^{-1}.

^{1}H NMR

^{1}H NMR spectra were recorded on Bruker AV-300C spectrometers at ambient temperature (300 K). ^{1}H spectroscopic chemical shifts δ are reported in ppm relative to tetramethylsilane. δ (^{1}H) were referenced internally to the relevant residual solvent resonances. For furan-functionalized polymers, Mn was calculated by setting the integral of the two β-hydrogen atoms of the bound furfuryl-moiety (6.50 ppm) to 4, because in the functionalized linear polymers there are two furfuryl-groups bound. For maleimide-functionalized polymers, the signal of the hydrogen atoms of the maleimide-ring was set to 4. The integral of the NH signals of the urethane groups could be used to calculate the repeating units and the molar mass.

Gel permeation chromatography (GPC)

To perform size exclusion chromatography, an amount of 50 mg of each sample was dissolved in 10 ml of tetrahydrofuran. Thereof, 40 µl was injected with an ASI-100 Automate Sample Injector of Dionex Corporation (Sunnyvale, CA). A narrow molecular weight distribution polystyrene standard (PSS Polymer Standards Service; Mainz, Germany) was used as calibration. The measurements were performed with a flow rate of 1 ml/min (Bischoff HPLC Compact Pump) at 40°C. Detection was performed with the Shimadzu (Kyoto, Japan) Refractive Index Detector RID-6A. The separation column used was the GPC/SEC-column SDV, linear M, 300 × 8 mm, 5 µm, 100 Å of PSS. The curves were examined with the PL Cirrus GPC/SEC Software (Version 1.2).

Rheological determination of the critical molecular weight (Mw [crit.])

Rheological measurements were performed using an Anton Paar (Graz, Austria) Rheometer with TruGap cone-plate geometry (1°–25 mm, $d = 0.049$ mm) and a peltier temperature control system at 85°C. The evaluation was carried out with the Rheoplus software 3.40. If necessary, the zero shear viscosity was determined after smoothing of the curve by Carreau–Yasuda simulation.

2.2 | Production of laminates

All adhesives were coated on corona treated (PET: 600 W m^{-5} min^{-1}, PE: 1,000 W m^{-5} min^{-1}; surface tension > 38 mN/m) DIN A4 films using the coating unit CUF 5 (Sumet Messtechnik, Denklingen, Germany) with 40 mm/s speed of application, and the integrated convective dryer was set to a temperature of 70°C and a drying time of 60 s. The adhesives were applied in the form of an ethyl acetate solution with a 30% solid content. For the target dry film thickness of 3.6 µm, a wired rod with 12.0 µm wet film thickness was used. The film materials used are PET (23 µm, Hostaphan), PE (45 µm, Hanita), and aluminum foil (20 µm).

The coating weight in g/cm^2 was determined by measuring the weight difference of a square 100 cm^2 coated film and the film after the removal of the adhesive and division through 100.

Subsequently to coating, a second film sheet (PET, PE, and aluminum) was laminated on the adhesive, using a hand-held roller. Each sample was cured both at room temperature and in an oven set at 60°C, under the pressure of a 5 kg weight.

Additional thickness measurements were performed with a precision thickness gauge FT3 with 0.1 µm resolution (Rhopoint Instruments, Beyhill on Sea, UK) at five random positions around the film testing area with a repetition accuracy of 0.5 µm. The values were averaged for further analyses.

2.2.1 | Differential scanning calorimetry (DSC)

DSC was performed on a DSC 821e instrument of Mettler-Toledo GmbH (Gießen, Germany) following the DIN EN ISO 11357-1 method. Specimens were heated from 23 to 200°C at a heating rate of 10 K min^{-1}. Two heating runs were performed with 6–10 mg of sample.

2.2.2 | Determination of curing time

The curing of the adhesives was tracked by infrared spectroscopy from the decrease of the maleimide signal at 696 cm^{-1}. The quantification of the reaction rate was done with the software Spectrum One by Perkin Elmer by correlating the intensity of the signal at 696 cm^{-1} with the intensity of the signal at 817 cm^{-1}. The intensity of the maleimide signal was divided by the intensity of the signal at 817 cm^{-1}. The time course over the curing time is shown in Table 5S.

2.2.3 | T-peel test

A Schenk-Trebel universal testing machine type RM 50 from Bischoff Prüftechnik GmbH (Solingen, Germany) was used for tensile testing. Before the measurement, the laminates were stored for at least 24 hr at 23°C and 50% relative humidity and cut into 15 mm wide strips. The test direction was perpendicular to the

laminating direction of the laminates. The angle between the nonseparated part and the machine direction was kept at 90°; test speed was adjusted to 50 mm/min. Five test specimens were used for each measurement. Since the measurement results were sometimes influenced by air bubbles and were therefore subject to fluctuations, constant ranges for determining the measurement values were selected if necessary with the aid of the Test&Motion program from Doli Elektronik GmbH (Münsingen, Germany).

2.2.4 | Statistical hypothesis testing

The five bond strength values obtained per laminate were subjected to a statistical analysis to evaluate significant differences in bond strength between the different laminates. Therefore, the Program Visual-XSel 12.0 Multivar (CRGRAPH, Munich, Germany) was used. For each laminate, the five values are first examined for normal distribution using the Anderson–Darling normality test, with a significance value of 0.05. A t-test was used to compare two laminates (e.g., to compare storage at room temperature and 60°C), provided that a normal distribution of the five samples was present in both cases. In cases where there was no normal distribution, the Wilcoxon U test was performed. For the simultaneous comparison of $n > 2$ laminates, the multi-t test was applied in the case of normal distributions, in the presence of a nonnormally distributed laminate the Mood's-Median Test. The significance level was set to .05 in each case.

2.3 | Recovery of the materials

The laminates were each cut into 20 square samples with dimensions of 1×1 cm. The samples were then placed in 100 ml DMSO, heated to 105°C and stirred with a 400 rpm stirring bar. The delamination process was followed by observation as well as by occasional sampling.

2.3.1 | FTIR

For IR measurements, a Fourier transform infrared spectrometer (L1280034) with the software Spectrum One by Perkin Elmer (Shelton, CT) was used. The instrument used in this study was the ATR (Golden Gate, Perkin Elmer, Shelton, CT) device. For one spectrum, ten scans were recorded. The wavenumbers in the mid-infrared region range from 4,000 to 600 cm^{-1}.

2.3.2 | Determination of the absorbed solvent by Headspace-GC

The experiments were performed on a CLARUS-500-TRAP with FID detector. The initial temperature was 50°C for 4 min and the sample was then heated to 320°C at 20°C/min and held for 5 min.

3 | RESULTS AND DISCUSSION

3.1 | Preparation of the functionalized prepolymers of different chain lengths and determination of the Mw (crit.)

First, the PU prepolymers of different lengths with maleimide/furan functionalization, which is necessary for the production of the DA adhesives, were prepared and analyzed. They were synthesized from the long-chain polyester diol Capa 2045, methylene diphenyl diisocyanate and furfuryl alcohol or N-HEMI in a procedure slightly modified to literature procedures.[24–27] By adjusting the ratio of the starting materials, the prepolymer was obtained in different chain lengths. In Table 1, an overview of the different compositions and the experimentally and theoretically determined molecular weight in each case are given. The experimental values were determined via GPC and ^{1}H NMR spectroscopy. In the ^{1}H NMR spectra, the molar mass was determined by normalizing the signals of the bound furans. The molecular masses resulted from the integrals of the N—H protons of the urethane groups. In this respect, it should be noted that polyester-PUs can form several hydrogen bonds in concentrated DMSO-d_6 solution and thus give several NH peaks in the ^{1}H NMR.[28] In the present case the NH in the urethane can form three hydrogen bonds (between NH and S=O if DMSO-d_6, NH and C=O-group of the Polyester-softsegment and NH and the C=O groups of the hardsegment.) This explains the two to three NH signals in the range of 9.6–9.4 ppm. The ^{1}H NMR spectra also show that no side reactions have occurred. Urea groups would be expected to appear in the high field shifted range, allophanate groups in the low field shifted range.[29,30]

The theoretical value was calculated using the Carothers equation,[31] assuming a conversion of $p = .99$. In addition, a theoretical molar mass was calculated from the equivalents of the individual adhesive components (Table 1).

The value determined by GPC tends to be slightly higher than the value determined by ^{1}H NMR. However, considering the results of the GPC measurement and that the measurement was performed with a polystyrene standard, the molecular weight seems to be overestimated due

TABLE 1 Overview of the compositions of the prepolymers produced and the molar masses determined by GPC, ^{1}H NMR or theoretical methods

Name	FFA	Capa	MDI	Mn from equivalents (g/mol)	Mn (theo)[31] ($p = .99$) (g/mol)	Mn$_{\text{GPC}}$ (g/mol)	M$_{\text{NMR}}$ (g/mol)
	2.0	n	1+n	$= 2 \cdot M_{\text{FFA}} + n \cdot M_{\text{Capa}} +$ $(1 + n) \cdot M_{\text{MDI}}$	$= \left(\frac{1 + \frac{n}{n+1}}{1 + \frac{n}{n+1} - 2\frac{n}{n+1}p} \right) \cdot M_0 + 2 \cdot M_{\text{FFA}}$	--	--
	2	1	2				
1F	2.0	2.0	3.0	2,047	4,044	3,193	2,136
2F	2.0	4.0	5.0.	3,648	5,481	5,656	3,963
3F	2.0	6.0	7.0	5,248	9,485	7,183	5,756
4F	2.0	8.0	9.0	6,849	11,924	9,050	8,009
5F	2.0	10.0	11.0	8,449	14,201	11,294	10,086
6F	2.0	13.0	14.0	10,850	17,344	16,958	13,629

Note: The theoretical molar mass was calculated using the Carothers equation and an assumed turnover of $p = .99$. Furthermore, it was calculated from the equivalents of the materials used.

to the deviating spatial behavior in the solution. The ratio between the ^{1}H NMR and GPC value is approximately 0.89 for the longer prepolymers. For the two shorter prepolymers, however, the GPC measurement provides significantly higher values deviating from the ratio of 0.89. This can be explained by the fact that short-chain polymers are at the end of the GPC calibration curve and, consequently, the values have relatively high uncertainty. In addition, the elution curves (compare Figure S15) show that the synthesis of the shortest polymer, 1F, produced a relatively high oligomer content. The oligomer content decreases with increasing molecular weight, which is explained by more isocyanate groups' ability to react due to the higher diol content.

The molecular masses determined by the Carothers equation slightly overestimated the molecular masses determined by ^{1}H NMR. This may be due to the fact that the assumed turnover of 0.99 for the calculation was not completely achieved. For the shorter polymers, the molar masses determined by ^{1}H NMR correspond almost exactly to the molar masses calculated from the ratio of the monomers used.

Based on the molecular weights determined by ^{1}H NMR, the critical molecular mass (M_c) was determined to ensure that the prepolymers had a molar mass that enabled entanglement and thus fulfilled a basic requirement for adhesion.[32] For this purpose, the zero shear viscosities of the furan-functionalized prepolymers were measured and applied double-logarithmically against the molar mass. Figure 2 shows that a slope of 3.13 is present for the prepolymers with a higher molecular mass than 3F. This slope is close to 3.4, the typical slope for molar masses above M_c. The slope between 0F and 1F is approximately 1.0, which is a typical slope for values below the critical molar mass. Thus, the Mw (crit.) is between 1F and 2F.[33]
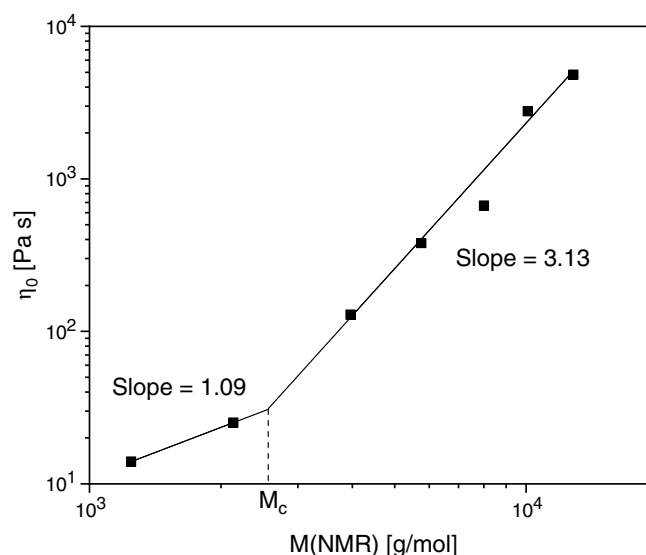

FIGURE 2 Estimation of the critical molar mass by double logarithmic application of the molar mass (determined by ^{1}H NMR spectroscopy) of the different prepolymers against the respective zero shear viscosity

For the laminate production, a chain length with a molar mass slight below the Mw (crit.) (1F) was selected and compared with the polymers above the Mw (crit.) (3F, 5F, and 6F). These prepolymers were each reacted with their corresponding maleimide-functionalized prepolymer (1M, 3M, 5M, and 6M) and a molecule carrying three-functional groups for cross-linking. The adhesives were formulated in such a way that equimolar amounts of furan and maleimide groups are present. In each formulation, about 50% of the furan groups are provided by the cross-linker molecule, the other half by the linear furan-functionalized prepolymer. Table 2 gives an overview of the formulations and their names.

TABLE 2 Overview of the adhesive formulations

Name	Furan-functionalized prepolymer		Maleimide-functionalized prepolymer		Crosslinking agent	
	Name (FX)	Eq.	Name (MX)	Eq.	Name	Eq.
Adhesive 1	F1	0.51	M1	1.00		0.33
Adhesive 2	F3	0.51	M2	1.00		0.33
Adhesive 3	F5	0.51	M3	1.00		0.33
Adhesive 4	F6	0.51	M4	1.00		0.33
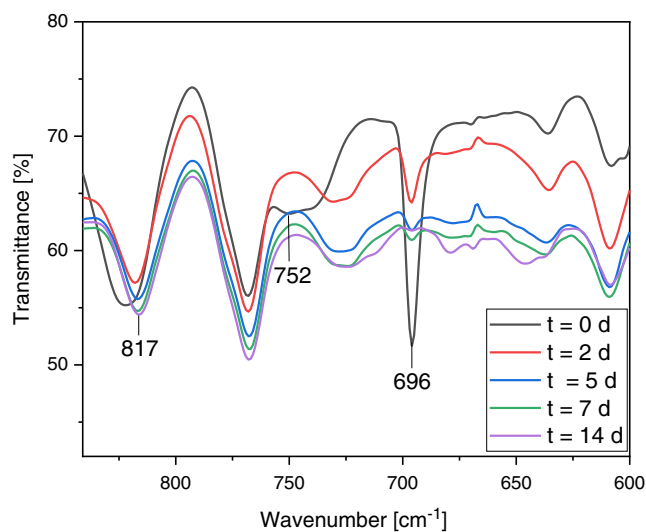
FIGURE 3 Monitoring of curing at various temperatures (IR) and determination of the exo/endo ratio (^{1}H NMR) [Color figure can be viewed at wileyonlinelibrary.com]

However, because shorter polymers have a relatively higher solubility compared with polymers with higher molecular weights,[34] faster laminate separation and thus a more efficient recycling process can be expected. In the special case of the use of 1F/1M, polymers above the critical molar mass are present in the adhesive due to the reaction between the two polymers. In the recycling process, however, the DA adducts open, which again results in polymers below the critical molar mass. This will further accelerate the delamination of the laminate.

The packaging relevant laminates PET//PE, PET//aluminum, and PE//aluminum and the additional laminate PET//PET, each with an adhesive layer thickness of 3–3.5 μm, were produced.

The curing of the adhesives was tracked by infrared spectroscopy from the decrease of the ring deformation mode of the maleimide at 696 cm^{-1} and the decrease of the absorption band of the furfuryl moiety at 752 cm^{-1}.[27] The curing process of Adhesive 1 at room temperature over 14 days is shown in Figure 3.

The relative height of the maleimide absorption band at 696 cm^{-1} to the constantly high absorption band at 817 cm^{-1} was used to estimate the rate of decrease of the maleimide groups and thus the curing rate. At 60°C and after 2 days, approximately 89% of all groups were converted, and at room temperature, approximately 70% of all groups were converted. The adhesive was completely cured after 3 days at 60°C and 14 days at room temperature. After this time, no further change in the maleimide absorption band was noticed.

A little residual signal could be noticed in some cases, which could be due to inaccuracies in the calculations caused by uncertainties in the estimation of molar masses. As expected, no difference in the curing time between the different prepolymer lengths could be observed.

However, curing at different temperatures changes the ratio between endo and exo adducts. To quantify this ratio, 1F and 1M were reacted without cross-linking agents and cured at both room temperature and 60°C. As expected, the samples cured at 60°C had a higher proportion of the thermodynamically more stable exo adduct (DA$_{exo}$:DA$_{endo}$; 5:1) (Figure 4b), whereas the sample stored at room temperature had a considerably higher proportion of the kinetically preferred endo adduct (DA$_{exo}$:DA$_{endo}$; 5:9) (Figure 4a).[16,35]

This finding is consistent with the results of the DSC measurements (see Figure S19). Furthermore, the evaluation of the DSC curves showed that the onset for the opening of the endo adduct takes place at around 80°C and at 115°C for the exo adducts. Due to the melting point of PE, the temperature in the recycling process should not exceed 105°C. Therefore, an excess of endo adducts would be beneficial for recycling.

3.2 | Adhesion

Before the laminates were recycled, adhesion measurements of the cured laminates were carried out using a T-peel test to validate the bonding.

In an ideal peel test, the peeling force increases to a certain extent depending on the adhesive strength of the
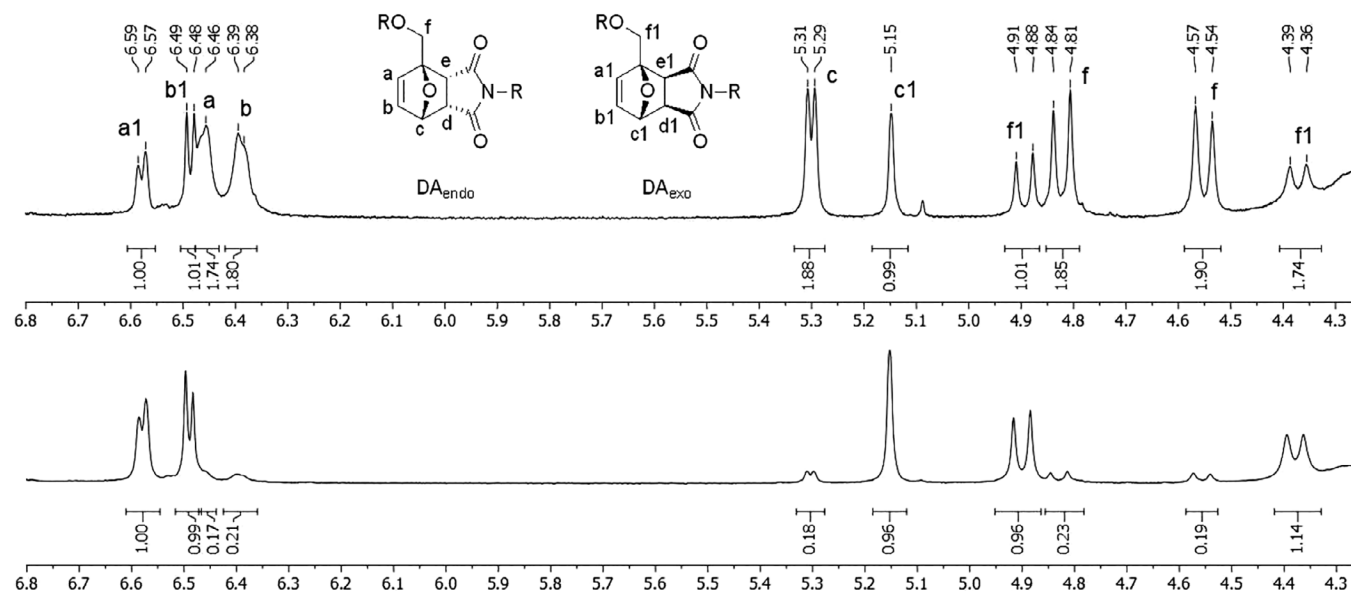
FIGURE 4   Excerpts of the ^{1}H NMR spectra of Adhesive 1 to estimate the exo/endo ratios: (a) shows that curing at room temperature provides an exo/endo ratio of about 1:1.8 and (b) shows that the exo/endo ratio obtained at 60°C is about 1:0.2

sample and then remains at a constant value. Figure 5 shows a typical force versus measurement distance curve obtained for a representative test specimen. Due to small inhomogeneities in the adhesive layer, such as air bubbles or small variations in the application thickness of the adhesive, which are often unavoidable during hand lamination, fluctuations in the determined force can be seen in many of the bond strength measurements. All measurement curves can be found in the Appendix. The mean values of the measurements (five samples each) are found in Table 2. In cases where material tearing in one of the substrate films (usually PET) occurred during measurement, no representative force was reported as the films often do not completely tear immediately, and therefore the values determined before the total tear are too low. In these cases, the bonding is stronger than the cohesion of the PET film.

To determine whether there were significant differences between the mean values given in Table 3, significant tests were carried out.

In the case of aluminum laminates, a significant decrease in adhesive strength was observed for longer prepolymers, whereas no significant differences were observed for pure plastic laminates. The reason for this is the viscosity of the 30% ethyl acetate solution in which the adhesive is applied, increases with increasing molecular weight. As a result, the adhesive is less able to penetrate surface irregularities of the aluminum foil and thus causes poorer adhesion.[36,37] The fact that longer polymers are theoretically capable of stronger entanglement is of no importance on metal surfaces. Contrarily, with
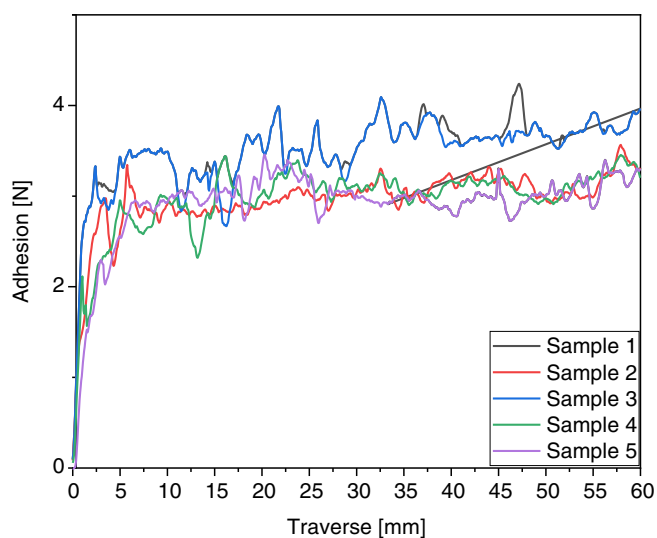

FIGURE 5   Typical curves of an adhesion measurement (5 samples/laminate) (in that case: Adhe. 2 PE/Alu, 60°C) without substrate failure. Fluctuations are due to inhomogeneities in the application (e.g., air bubbles) [Color figure can be viewed at wileyonlinelibrary.com]

polymer substrates, entanglement plays an important role in adhesion. This could explain why the measured bond strengths of the PET//PET and PET//PE composites increase with an increasing chain length or remain comparable despite increasing viscosity.

Furthermore, the use of prepolymers of different lengths changes the degree of cross-linking and the ratio between flexible and rigid structures in the adhesive.

TABLE 3 Mean values and standard deviations of the bond strength measurements related to the 15 mm width of the test strips

	PET//PET		PET//PE		PET//Alu		PE//Alu	
	rt	60°C	rt	60°C	rt	60°C	rt	60°C
1M/1F	Tear of PET	Tear of PET	2.10 ± 0.08 N	3.00 ± 0.14 N	2.05 ± 0.06 N	1.95 ± 0.27 N	$2.3\,1 \pm 0.01$ N	3.15 ± 0.14 N
3M/3F	Tear of PET	Tear of PET	3.26 ± 0.09 N	Tear of PET	2.16 ± 0.11 N	2.25 ± 0.21 N	2.38 ± 0.13 N	3.18 ± 0.28 N
5M/5F	1.52 ± 0.12 N	1.56 ± 0.15 N	2.12 ± 0.07 N	Tear of PET	0.39 ± 0.05 N	0.79 ± 0.08 N	0.89 ± 0.11 N	1.57 ± 0.02 N
6M/6F	3.17 ± 0.39 N	3.08 ± 0.16 N	2.58 ± 0.18 N	Tear of PET	0.79 ± 0.08 N	0.66 ± 0.05 N	1.04 ± 0.20 N	1.65 ± 0.12 N

Note: The numerical values indicate the mean value from five measurements. All measurement curves can be found in the Supporting Information.
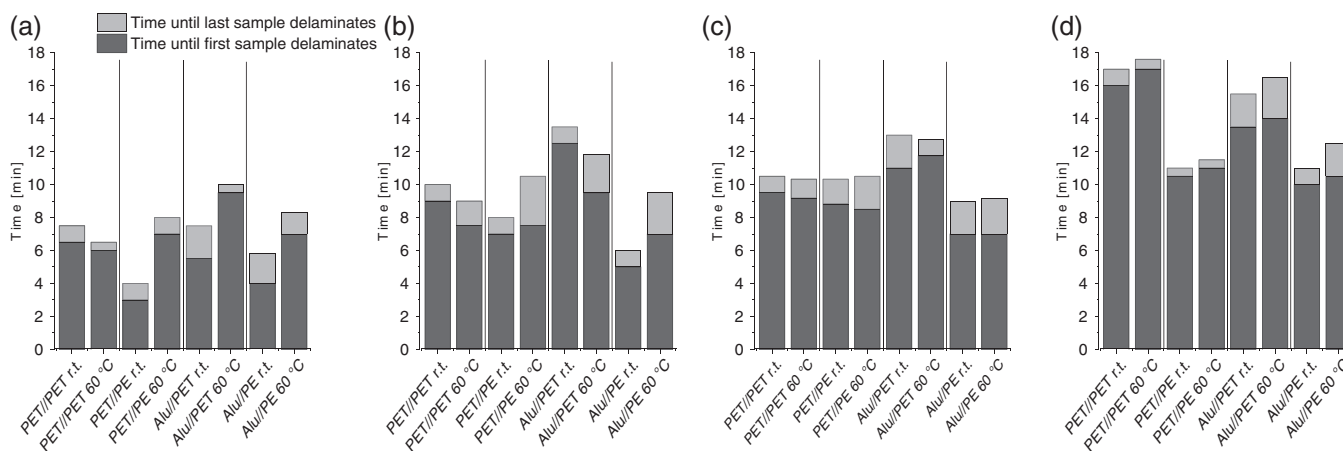

FIGURE 6 Schematic representation of the delamination process. The filled arrows symbolize the dissolution process of the adhesive components over the cutting edge of the laminate pieces. The unfilled arrows symbolize the permeation of the solvent through the PE film, which also causes an early start of the dissolution process in the middle of the sample pieces

In some cases, laminates cured at 60°C showed significantly higher adhesive strength than those cured at room temperature. This could be due to the improved surface contact of the adhesive during the curing process as polymers are less viscous at 60°C and can therefore form more intermolecular interactions with the surface of the substrates.[36,38] The higher mobility of polymer chains at elevated temperatures could contribute to a stronger entanglement with the polymers of the substrates and thus to a stronger adhesion.[36] In the case of a PU adhesive containing polyester, it is expected that PET laminates would exhibit greater adhesion than PE laminates due to the greater structural similarity and the resulting stronger intermolecular interactions. In the present experiments, this could not be determined. Instead, the adhesion of PET and PE laminates appears to be comparable, or even stronger, for PE laminates.

3.3 | Delamination

After the T-peel test had confirmed the adhesion of the laminates, the films were made available for recycling by delamination. The delamination of the laminates was performed with 1 cm^2 flakes at 105°C in DMSO under moderate shearing. The temperature was chosen so that the temperature would be as high as possible to allow a retro-DA reaction to take place, but the PE should still be dimensionally stable. DMSO was chosen because of its satisfactory solubility of the prepolymers and its high boiling point, which allows the retro-DA reaction to be carried out.

To determine the minimum dissolution time of the polymers, delamination experiments were first carried out with laminates, which were only prepared with furan-functionalized prepolymers (1F–6F). For practical reasons, PET//PET laminates were used. As expected, the delamination times of the composites increased with increasing chain length (1F 5:30 min, 2F 6:30 min, 3F 7:20 min, 4F 8:00 min, 5F 9:30 min, and 6F 11:00 min).

This trend is also evident in the cross-linked adhesives (Figure 6), although some PE laminates have lower dissolution times than pure, noncross-linked prepolymers in PET//PET laminates. In general, the type of laminate also influences the delamination duration. Composites that do not contain PE tend to have longer dissolution times.

FIGURE 7 Graphical representation of the delamination times of the various composites. The bars with the close-meshed pattern symbolize the time until the delamination of the first samples can be observed. The bars with the wide-meshed pattern symbolize the time until the delamination of the last sample can be observed: (a) shows the results of Adhesive 1, (b) Adhesive 2, (c) Adhesive 3, and (d) Adhesive 4 [Color figure can be viewed at wileyonlinelibrary.com]

In PET-containing laminates, it can be observed that the adhesive is removed from the outside cutting edges. The samples can only be moved mechanically against each other shortly before complete delamination because the adhesive is hardly influenced in the middle of the laminate nips before. Especially with PET//aluminum laminates, the adhesion in the middle of the laminate slice is maintained for a relatively long time. With PE//aluminum composites, the two films can be shifted more quickly against each other and the adhesion in the middle decreases more quickly.

These observations can be explained by the barrier properties of PET and PE. The diffusion coefficient of organic solvents for PE is significantly higher than for PET,[39] especially because the test temperature of 105°C is almost in the melting range of PE. Thus, in the case of PET, the solvent primarily penetrates the adhesive via the cut edges, whereas in the case of PE, the solvent can also permeate through the film (Figure 7).

As was to be expected, samples cured at 60°C tend to have a longer delamination time than samples stored at room temperature. The effect, however, was less significant than expected. Generally, the significantly higher proportion of exo adduct would lead to a longer delamination time due to the higher activation energy for the retro-DA reaction. However, in both cases, enough adducts seem to be opened at 105°C to allow dissolution of the adhesive by DMSO. By means of DSC, an onset for the retro reaction of the endo adduct of 80°C and the exo adduct of 115°C was determined. However, according to Froidevaux et al.,[16] the temperature of the retro-DA reaction of the endo adduct is lower and the DSC analysis is not an appropriate analytical tool to precisely detect the onset of the retro-DA reaction. Moreover, in the retro-DA reaction of the exo adduct, the onset may not be accurately determined due to signal overlaps.

However, in all cases, it must be taken into account that the determined delamination times are subject to a certain degree of uncertainty as it is sometimes visually difficult to determine the exact delamination time.

3.4 | Recovery of monomaterials and characterization

After complete delamination, the monomaterial films (PET, PE, and aluminum) were suspended separately. As
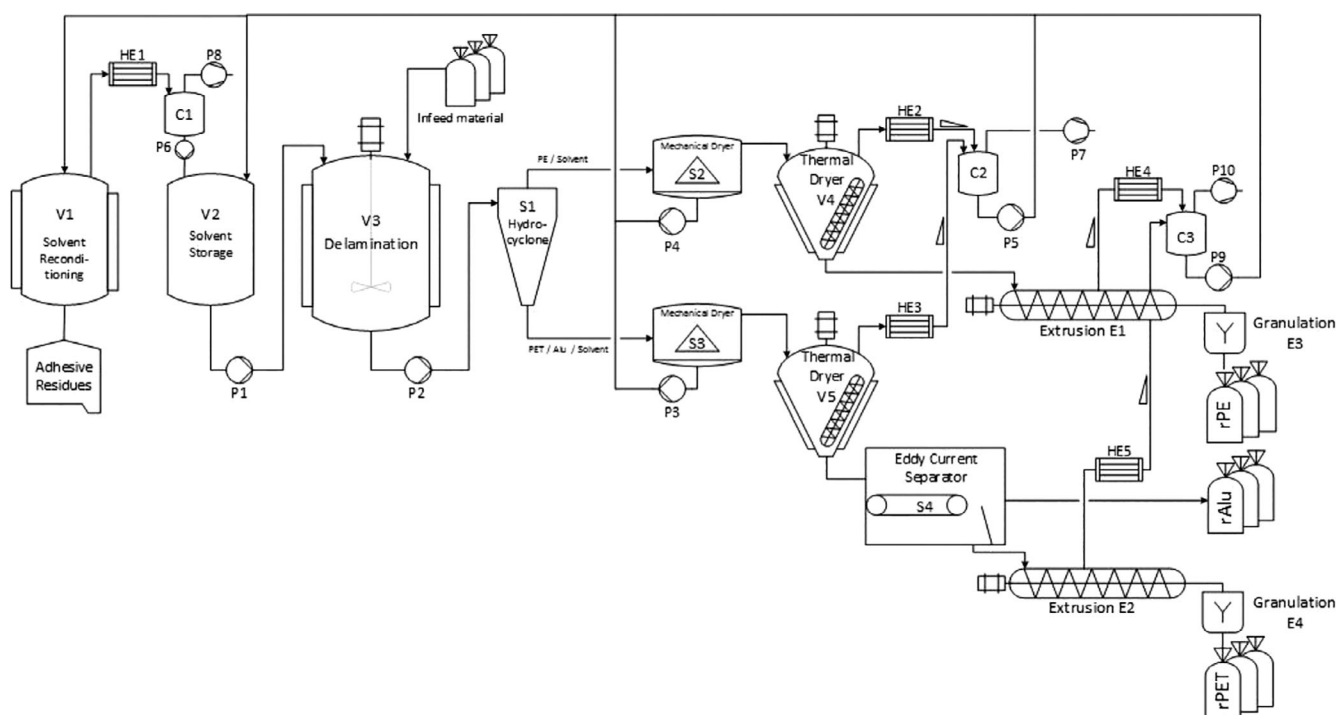

FIGURE 8 Possible process flow diagram for implementation. C, catchpot; E, extrusion incl. Granulation; H, heat exchanger; P, pump; S, separator; and V, vessel

PE has a density of lower than 1 g/cm³, it floats on the surface of DMSO and can be easily separated from the sinking materials PET and aluminum. The adhesive components were solvated and could no longer be detected by IR spectroscopy on the surface of the films (see Supporting Information Figure S22 and Figure S23). Headspace-GC was used to determine the amount of solvent absorbed by the PE/PET films. The results of 4.5 ppm for PE and 2.1 ppm for PET show that extrusion degassing would be necessary for further processing of the two monomaterial polymer streams. The following chapter describes a possible process flow diagram of the upscaled recycling process (Figure 8).

3.5 | Process flow diagram

The delamination process is carried out in a heated vessel, connected to a solvent reservoir and an infeed for the material to be treated. A hydrocyclone is suitable for density separation of the flakes obtained after delamination, in which PE can be separated from PET and aluminum. A predrying of the respective three material fractions can be achieved mechanically by a decanter centrifuge. The subsequent thermal drying can be carried out via a vacuum dryer that ensures a low residual solvent content of down to 1%.

The aluminum can then be removed from the PET// aluminum fraction by an eddy current separator or electrostatic separation. Reextrusion of the PET and PE-fraction is then carried out under degassing.

The solvent recovered by mechanical/thermal drying and degassing can, due to the low concentration of monomers in solution, be used again directly for delamination for $n > 10$ rounds before a distillation of the solvent would become necessary.

An additional recovery of the adhesive is not aimed at, as this would be difficult to achieve on the one hand and impurities such as printing inks would be contained in the distillation sump under real conditions.

4 | CONCLUSIONS

Multilayer packaging is an effective way to protect food items, but it remains under criticism as it is not recyclable. New technologies, such as debondable adhesives, are an option to address this problem. This research article has shown that producing typical packaging laminates with PU adhesives containing DA adducts is possible. Subsequently, these laminates can be delaminated into individual materials by treating the size-reduced composite material with a heated solvent. Although there are different ratios between endo and exo adduct in the adhesives due to different curing temperatures, no significant difference in delamination times could be observed. Instead, differences in the barrier properties of the respective film materials and longer prepolymers have an influence on delamination times. However, as the difference between the dissolution times is in the minute range, the longer dissolution times do not hinder the feasibility.

The materials obtained after delamination no longer exhibited adhesive residues and can be made accessible for recycling as a pure material through density separation or eddy current separation.

With regard to the material characterization of the laminates, a future scale-up to machine lamination will be advantageous because defects and the standard deviation of the bond strength measurements can be reduced. To use this method for the production of recyclable multilayer packaging, it is necessary to use only raw materials that are harmless from a food law point of view. Further research that includes this aspect will be published.

CONFLICT OF INTEREST
The authors declare no potential conflicts of interest.

ORCID
Katharina M. A. Kaiser https://orcid.org/0000-0002-9810-3416

REFERENCES
[1] _European Comission, A European Strategy for Plastics in a Circular Economy_, **2018**.
[2] A. Nonclercq, _Mapping Flexible Packaging in a Circular Economy [F.I.A.C.E]: Final report_, **2016**.
[3] J. Dixon, Packaging materials: 9. in _Multilayer Packaging for Food and Beverages_, International Life Sciences Institute, Washington D.C. **2011**.
[4] P. Singh, A. A. Wani, H.-C. Langowski Eds., _Food Packaging Materials: Testing & Quality Assurance_, CRC Press Tayöpr & Francis Group, Boca Raton, London, NY **2017**.
[5] K. Kaiser, M. Schmid, M. Schlummer, _Recycling_ **2018**, _3_, 1.

[6] G. Bleisch, H.-C. Langowski, J.-P. Majschak, *Lexikon Verpackungstechnik*, Behr, Hamburg **2014**.

[7] Die Pla.to GmbH und die Hochschule Zittau/Görlitz entwickeln ein innovatives Recyclingverfahren für die Trennung von Folien aus Altverpackungen, **2019**.

[8] T. Manouras, M. Vamvakaki, *Polym. Chem.* **2016**, *8*, 74.

[9] D. G. Bekas, K. Tsirka, D. Baltzis, A. S. Paipetis, *Compos. B: Eng.* **2016**, *87*, 92.

[10] T. Hughes, G. P. Simon, K. Saito, *Mater. Horiz.* **2019**, *6*, 1762.

[11] C. P. Kabb, C. S. O'Bryan, C. C. Deng, T. E. Angelini, B. S. Sumerlin, *ACS Appl. Mater. Interfaces* **2018**, *10*, 16793.

[12] P. Du, X. Wang, in *Recent Advances in Smart Self-Healing Polymers and Composites*, Vol. 58 (Eds: G. Li, H. Meng), Elsevier/WP Woodhead Publishing, Amsterdam, Boston, Cambridge **2015**, p. 159.

[13] S. K. Ghosh, *Self-Healing Materials: Fundamentals, Design Strategies, and Applications*, Wiley-VCH, Weinheim **2009**.

[14] A. V. Menon, G. Madras, S. Bose, *Polym. Chem.* **2019**, *10*, 4370.

[15] G. Li, H. Meng Eds., *Recent Advances in Smart Self-Healing Polymers and Composites*, Elsevier/WP Woodhead Publishing, Amsterdam, Boston, Cambridge **2015**.

[16] V. Froidevaux, M. Borne, E. Laborbe, R. Auvergne, A. Gandini, B. Boutevin, *RSC Adv.* **2015**, *5*, 37742.

[17] I. C.-Y. Hou, Y. Hu, A. Narita, K. Müllen, *Polym. J.* **2018**, *50*, 3.

[18] M. A. Tasdelen, *Polym. Chem.* **2011**, *2*, 2133.

[19] A. Gandini, *Polymer* **2005**, *15*, 95.

[20] Y.-L. Liu, T.-W. Chuo, *Polym. Chem.* **2013**, *4*, 2194.

[21] Z. Karami, F. Nademi, M. J. Zohuriaan-Mehr, A. Rostami, *J. Appl. Polym. Sci.* **2017**, *134*, 3094.

[22] N. I. Khan, S. Halder, S. B. Gunjan, T. Prasad, *IOP Conf. Ser.: Mater. Sci. Eng.* **2018**, *377*, 12007.

[23] G. Oertel, G. W. Becker, D. Braun Eds., *Polyurethane; Mit 126 Tabellen*, München, Hanser **1993**.

[24] Y. Heo, H. A. Sodano, *Adv. Funct. Mater.* **2014**, *24*, 5261.

[25] H.-Y. Duan, Y.-X. Wang, L.-J. Wang, Y.-Q. Min, X.-H. Zhang, B.-Y. Du, *Macromolecules* **2017**, *50*, 1353.

[26] P. Buono, A. Duval, L. Averous, Y. Habibi, *Polymer* **2017**, *133*, 78.

[27] D. H. Turkenburg, H. van Bracht, B. Funke, M. Schmider, D. Janke, H. R. Fischer, *J. Appl. Polym. Sci.* **2017**, *134*, 26.

[28] X. Lu, Y. Wang, X. Wu, *Polymer* **1994**, *35*, 2315.

[29] A. M. Heintz, D. J. Duffy, S. L. Hsu, W. Suen, W. Chu, C. W. Paul, *Macromolecules* **2003**, *36*, 2695.

[30] M. Sumi, Y. Chokki, Y. Nakai, M. Nakabayashi, T. Kanzawa, *Makromol. Chem.* **1964**, *78*, 146.

[31] A. Rudin, P. Choi, *The Elements of Polymer Science and Engineering*, Academic Press, Waltham, MA **2013**.

[32] S. J. Abbott, *Adhesion Science: Principles and Practice*, DEStech Publications, Lancaster, PA **2015**.

[33] M. M. Cross, *Polymer* **1970**, *11*, 238.

[34] B. A. Miller-Chou, J. L. Koenig, *Prog. Polym. Sci.* **2003**, *28*, 1223.

[35] L. Rulísek, P. Sebek, Z. Havlas, R. Hrabal, P. Capek, A. Svatos, *J. Org. Chem.* **2005**, *70*, 6295.

[36] D. E. Packham, in *Handbook of Adhesion Technology* (Eds: L. F. M. da Silva, A. Oechsner, R. D. Adams), Springer International Publishing, Basel, Germany **2019**, p. 1.

[37] A. J. Kinloch, *Adhesion and Adhesives: Science and Technology*, Chapman & Hall, London **1994**.

[38] G. Habenicht, *Kleben: Grundlagen, Technologien, Anwendungen*, Springer-Verlag Berlin Heidelberg, Berlin, Heidelberg **2009**.

[39] P. Dole, A. E. Feigenbaum, C. de la Cruz, S. Pastorelli, P. Paseiro, T. Hankemeier, Y. Voulzatis, S. Aucejo, P. Saillard, C. Papaspyrides, *Food Addit. Contam.* **2006**, *23*, 202.

SUPPORTING INFORMATION

Additional supporting information may be found online in the Supporting Information section at the end of this article.